Journal of Analytical Science and Technology
a SpringerOpen Journal

RESEARCH Open Access

Synthesis of alumina, titania, and alumina-titania hydrophobic membranes via sol–gel polymeric route

Amany Abd AL-Azem Gaber[1*], Doreya Mohamed Ibrahim[1], Fawzia Fahm Abd-Almohsen[2] and Elham Mohamed El-Zanati[3]

Abstract

Nanometer TiO_2-Al_2O_3 composite membranes were synthesized through the sol–gel polymeric reaction of $TiCl_4$ and $AlCl_3$ in the presence of acrylic-acrylamide copolymer as a template. The dried samples were characterized by DTA, TGA, FTIR, XRD, and TEM to determine the thermal behavior, chemical composition, crystal structure, shape, and size of the particles. Octyltrichlorosilane was chosen as a silane coupling agent to increase the hydrophobic nature of the prepared membranes. The morphological structure, hydrophobic nature, water permeability, and desalination efficiency of the prepared membranes were studied by SEM, contact angle, permeability, and NaCl rejection coefficient (*R*%) measurements. The crystal structure of titania and alumina particles in the composite was affected by the $AlCl_3$ and $TiCl_4$ feed ratio. As the titania concentration increased, the average particle size of the composite particles became larger and the uniformity of the membrane layer decreased. The alumina (75%)-titania (25%) composite (AT25) showed a uniform crack-free membrane layer with a pore diameter of 12.9 nm and a porosity of 21.46%, with great hydrophobic nature, and with contact angle reaching 116°. This membrane can withstand calcination temperature up to 700°C, as the alumina and titania were present in their active forms: gamma-alumina and anatase, respectively. The membrane produced from this composite showed a high surface area of 333 m^2/g with a respective particle size of 4.6 nm. Moreover, it showed a high ability to reject NaCl from water with a rejection coefficient of 73% and a high permeation flux of 4.8 l/h m^2 at 75°C.

Background

Ceramic membranes are gaining more and more importance in separation technology, especially in combination with catalytic processes. They have several positive merits especially their chemical resistance, thermal resistance, and high permeability (Schaep et al. 1999; van Gestel et al. 2002, 2003). The main aim of the research work in this field was the production of new nano-porous metal oxide membranes. Thus, great advances were made regarding the development of non-silicate ceramic membranes. Systems like ZrO_2 and TiO_2 were taken into consideration, in particular with respect to their chemical resistance (Schaep et al. 1999; van Gestel et al. 2002, 2003; Shojai and Mantyla 2001). Also, γ-Al_2O_3 and TiO_2 were of main interest (Xu and Anderson 1993; Larbot et al. 1994; Wildman et al. 1994; Puhlfürß et al. 2000). These membranes have high selectivity against small macromolecules. The reduction in pore size from ultrafiltration to nano-filtration range was enabled by changing the method of synthesis and the precursors used from the colloidal to the polymeric sol–gel technique.

Alumina membranes based on the application of a template polymer were produced over decades (Benfer et al. 2001; Richter et al. 1997; Benfer et al. 2004) with varying pore sizes and permeation rates. However, there was a current limitation for the practical application of these alumina membranes due to the failure in the production of a complete crack-free layer by the sol–gel technique. The partial kinetic γ- to α-alumina phase transformation occurs upon calcination of the alumina membrane layer at temperatures above 600°C. Phase transformation takes place by coalescence of small (γ-alumina) particles into

* Correspondence: amany1gaber@yahoo.com
[1]Ceramic Department, National Research Centre, Cairo, Egypt
Full list of author information is available at the end of the article

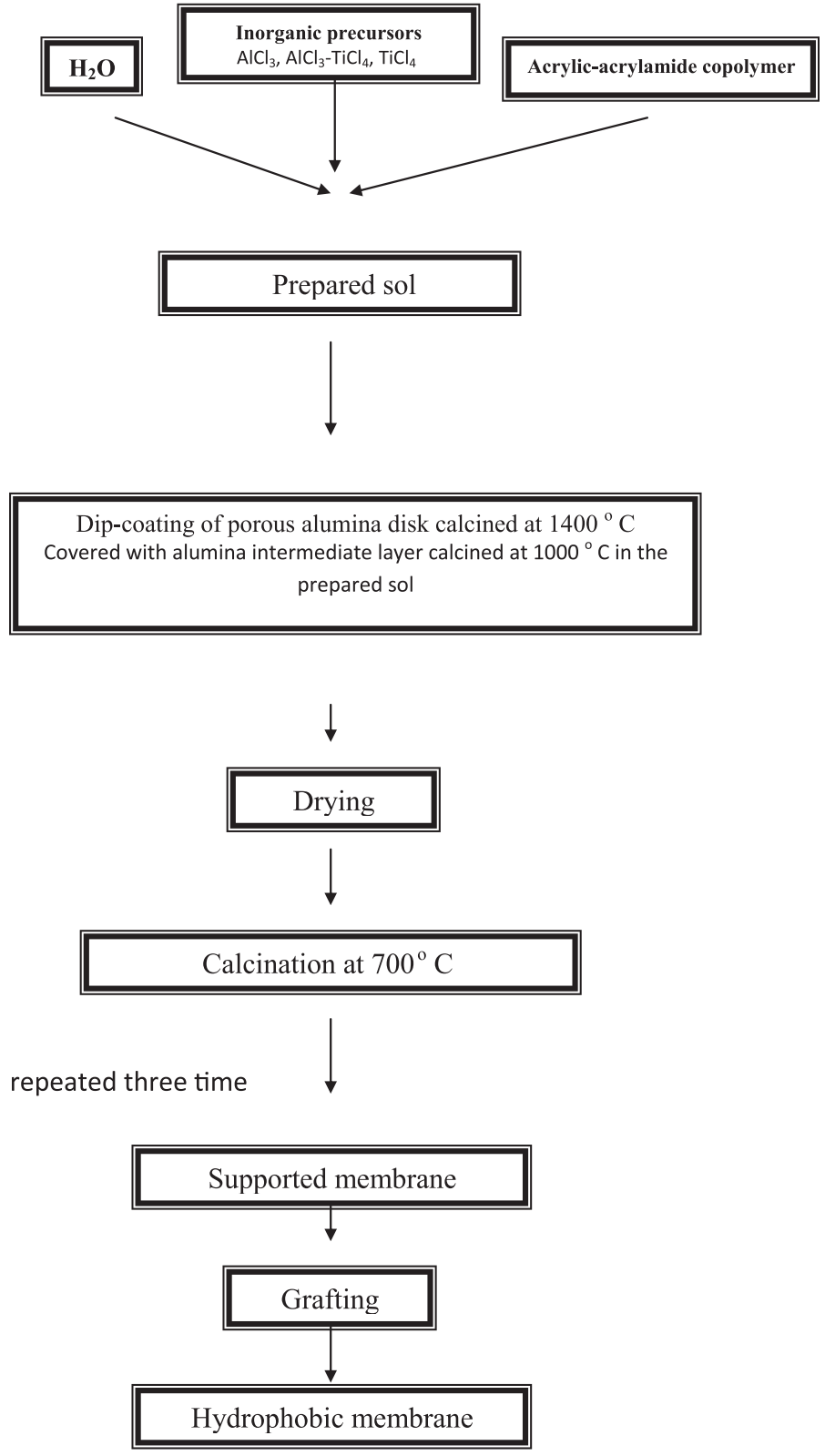

Figure 1 Steps of hydrophobic membrane layer preparation.

larger (α-alumina) grains, accompanied by considerable grain and pore growth. This was practically overcome by calcination at a minimum temperature of 600°C to obtain well-defined, mechanically stable layers of alumina membranes (Gaber 2007). The effect of phase transformation and accompanying grain growth can be avoided as suggested by Kumar, by retarding its occurrence to a temperature above the normal calcination temperature. It has been suggested that the presence of a second phase decreases the sub-coordination number of the prepared particles in the nano-composite matrix (Sekulic et al. 2004; Kumar 1993; Zhang and Banfield 1999). The presence of titania as a second phase to form an alumina-titania composite membrane retards the γ-alumina transformation and keeps it in its amorphous phase, avoiding its transformation into α-alumina phase; at the same time, the presence of alumina keeps the titania in its stable form as anatase phase.

The present work aims at preparing alumina-titania composite membranes that can withstand temperature up to 700°C. The prepared membrane surfaces were modified by octyltrichlorosilane to render them hydrophobic for desalination purposes. The properties and microstructure of the prepared membranes before and after modification were characterized.

Methods

Materials

Pure chemical reagents were selected to prepare the required membranes. The following precursors were used: aluminum chloride ($AlCl_3$) was supplied by Aldrich (St. Louis, MO, USA), titanium chloride ($TiCl_4$) by Fluka Chemika (Buchs, Swizerland), aluminum hydroxide ($Al(OH)_3$) by Arabian Medical & Scientific Lab. Sup. Co. (Dubai, United Arab Emirates), ammonium persulfate and acrylic and acrylamide monomers by Merk-Schuchardt (Darmstadt, Germany), polyvinyl alcohol by German, and octyltrichlorosilane by Aldrich.

Method of preparation of the membranes

The method of membrane preparation is demonstrated by the flow chart in Figure 1.

Preparation of the acrylic-acrylamide copolymer

Acrylic-acrylamide was polymerized on laboratory scale via a free radical method to obtain the copolymer Gaber AA (2007). Preparation of alumina membranes by sol–gel polymeric route 658 M.Sc Thesis, Cairo University. The following shows the reaction of formation:

$$\begin{array}{ccc} \text{Acrylic acid monomer} & + & \text{Acrylamide monomer} \\ n\,CH_2 = \text{CH-COOH} & & n\,CH_2 = \text{CH-CO-NH}_2 \\ & \downarrow & \\ & [\text{Acrylic-acrylamide copolymer}]_n & \end{array}$$

Table 1 Composition of the prepared membranes

Membrane symbol	Type of inorganic salts	Concentration of inorganic salts (mol%)
A	$AlCl_3$	100% $AlCl_3$
T	$TiCl_4$	100% $TiCl_4$
AT25	$AlCl_3$-$TiCl_4$	75% $AlCl_3$
		25% $TiCl_4$
AT50	$AlCl_3$-$TiCl_4$	50% $AlCl_3$
		50% $TiCl_4$
AT75	$AlCl_3$-$TiCl_4$	25% $AlCl_3$
		75% $TiCl_4$

Preparation of the alumina support

Supports in the form of disks with the following dimensions: diameter 25 mm and thickness 2 mm, were processed from α-alumina powder (commercial alumina) with a mean particle size ≤10 μm and 2 wt% polyvinyl alcohol as organic binder under a uniaxial press and a pressure of 200 MPa. The specimens were dried and then first fired in a muffle furnace in air at a rate of 2°C/min up to 500°C and maintained for 2 h at this temperature to eliminate the organic binder. Heating was then continued at a rate of 4°C/min up to 1,400°C for 4 h and then cooled to room temperature.

Preparation of the alumina suspension

Fine α-alumina powder was first prepared by calcining chemically pure $Al(OH)_3$ at 1,200°C for 3 h. The obtained powder was used to prepare a homogeneous and stable suspension by the addition of 0.5 ml of ammonia solution, 10 g of acrylic-acrylamide copolymer, and 6.6 g of 3.5 wt% polyvinyl alcohol solution; 1.08 g of this dispersing agent was added to 1 g of the calcined α-alumina powder and well stirred for 1 h, followed by dispersing in an ultrasonic bath for another 1 h.

The prepared suspension was poured on the surface of the alumina support, homogenized to form a uniform layer of about 3 μm thick, dried for 24 h at 80°C, and then fired at 1,000°C for 3 h at a heating rate of 1.5°C/min.

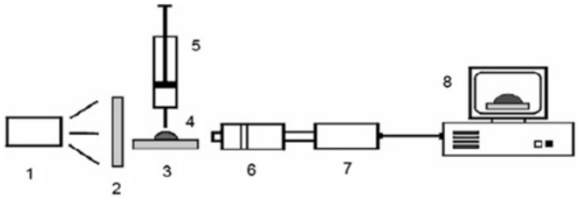

Figure 2 A block diagram of an apparatus for measuring ceramic membrane wettability. 1 - light source, 2 - diffuser, 3 - measuring Table, 4 - liquid droplet, 5 - manual syringe, 6 - camera lenses, 7 - CCD camera, 8 - PC with an image acquisition card and image processing applications (University of Alabama).

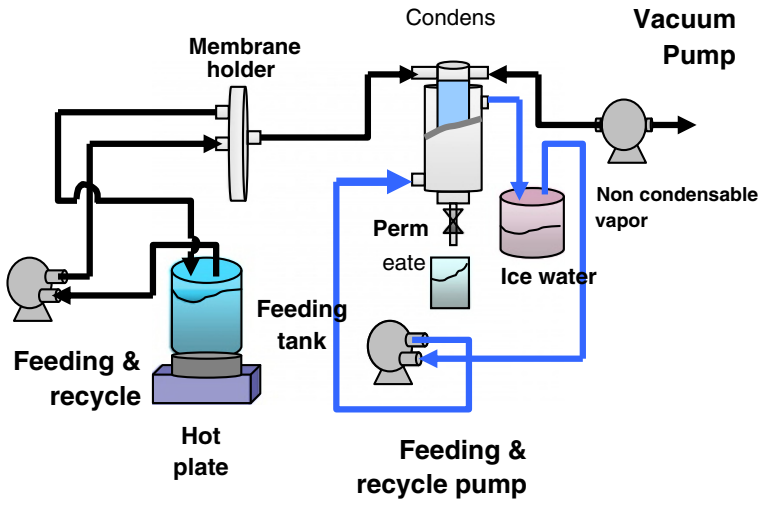

Figure 3 Vacuum membrane distillation system (flow diagram).

Preparation of the membrane layer

The salt solution of $AlCl_3$ and $TiCl_4$ (alumina 100% and titania 100%) as well as $AlCl_3$-$TiCl_4$ mixed oxides (75%:25%, 50%:50%, and 25%:75%) were prepared by dissolving the calculated ratio equivalent to 12 mol. The prepared solid solutions were added dropwise to an equivalent weight of 1 mol of the acrylic-acrylamide monomer that was kept constant in all batches as demonstrated in Table 1. The reaction proceeds at room temperature in an acidic media at pH 3 with continuous

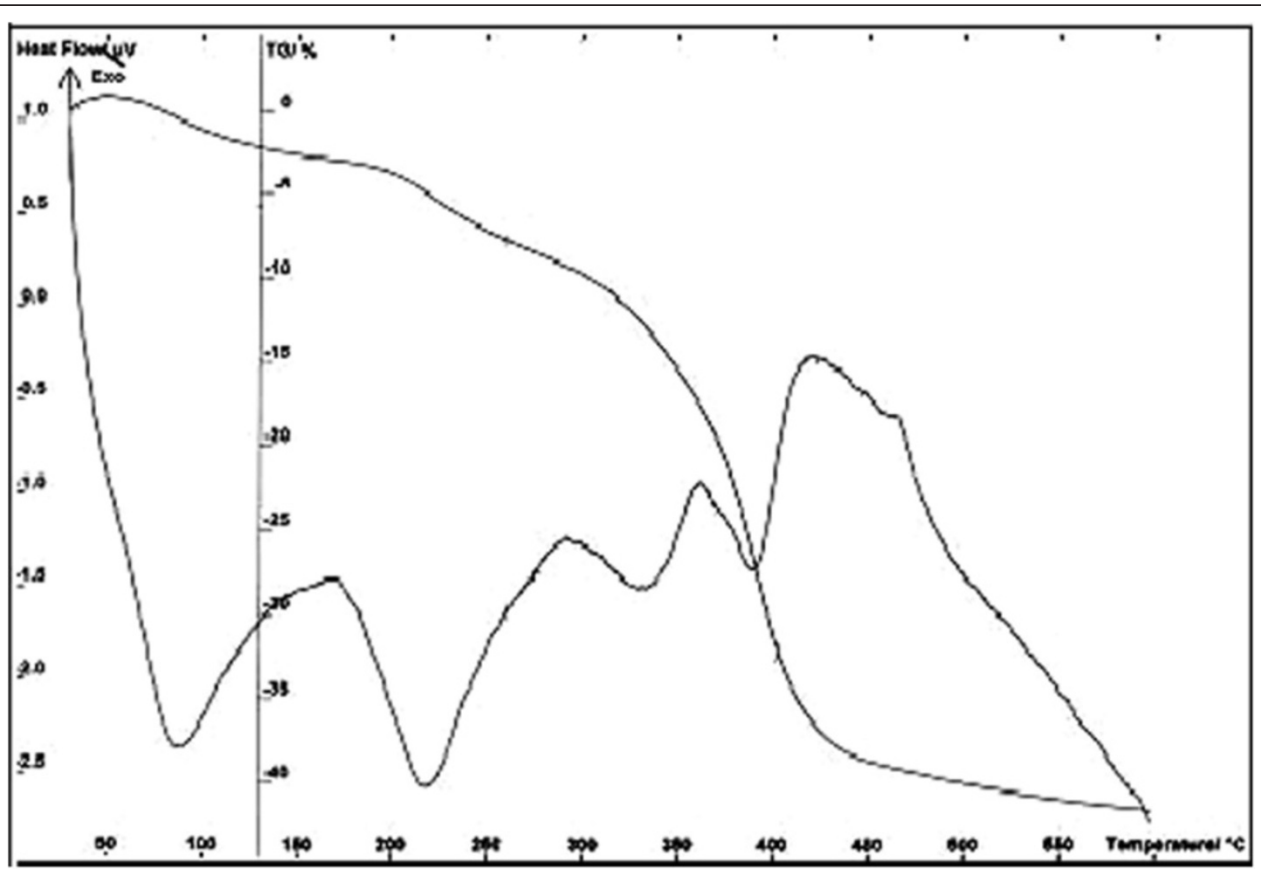

Figure 4 Thermal analysis of the acrylic-acrylamide copolymer.

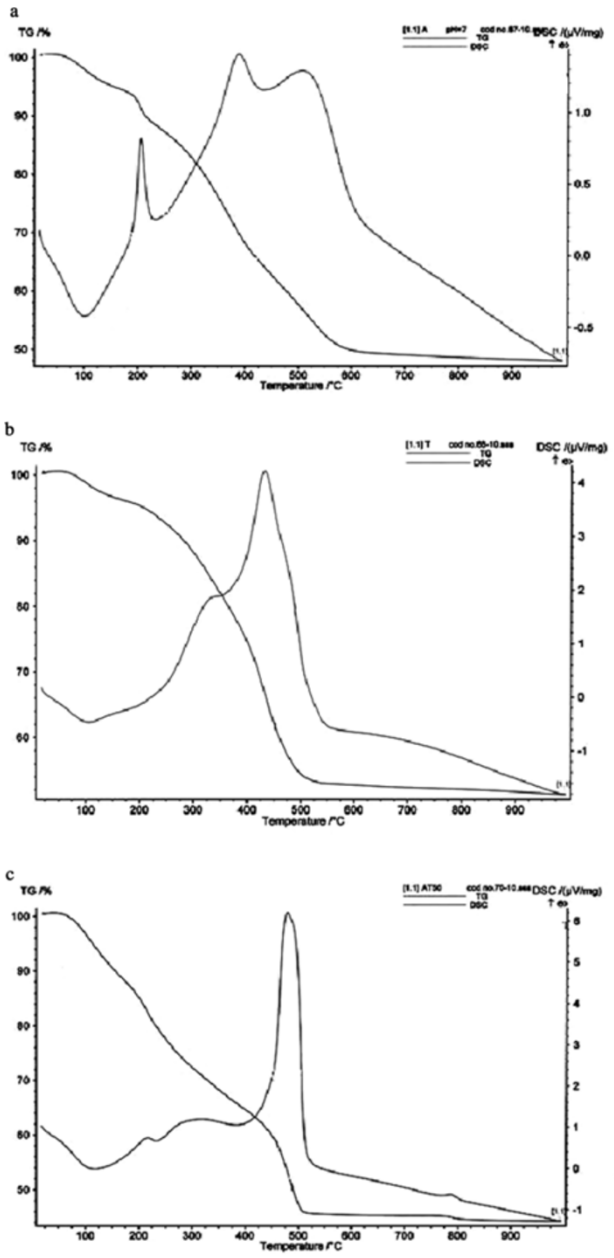

Figure 5 DSC and TGA curves of acrylic-acrylamide copolymers incorporated with (a) Al^{3+} (A), (b) Ti^{4+} (T), and (c) Al^{3+}-Ti^{4+} (AT50).

Table 2 Temperatures of the DSC peaks of the free polymer and those incorporated with Al^{3+} and Ti^{4+}

Material	Endothermic peak temperature (°C)				Exothermic peak temperature (°C)			
	First	Second	Third	Fourth	First	Second	Third	Fourth
Free polymer	85	217	334	389	420	-	-	-
+Al^{3+}	102	-	-	-	207	388	508	-
+Al^{3+} and Ti^{4+}	118	232	-	-	479	787	-	-
+Ti^{4+}	106	-	-	-	433	-	-	-

Table 3 Temperatures of the main weight loss steps in the TGA curves of the polymers

Material	Main steps							
	Step I		Step II		Step III		Step IV	
	Temperature (°C)	Weight loss (%)	Temperature (°C)	Weight loss (%)	Temperature (°C)	Weight loss (%)	Temperature (°C)	Weight loss (%)
Free polymer	50 to 179	8	179 to 218	12	308 to 450	80		
$+Al^{3+}$	75 to 162.5	5.8	163 to 242.5	6.6	243 to 637	38.77	637 to 1,000	16.26
$+Al^{3+}$ and Ti^{4+}	50 to 175	12	175 to 378	22.3	378 to 550	20.42	775 to 1,000	1.27
$+Ti^{4+}$	75 to 175	4.4	175 to 375	14.4	375 to 570	28.7	570 to 1,000	1.57

stirring. A gel layer was deposited on the surface of the support by a dipping procedure. The obtained gel layers were left to dry at room temperature for 24 h followed by drying for 24 h at 80°C. Finally, calcination of the prepared membranes took place at 700°C for 3 h in a temperature-programmable furnace with heating and cooling rates of 1.5°C/min. The deposition of the membrane layer was repeated three times as demonstrated in the flow chart in Figure 1.

Grafting process

Organo-silane products are used in surface modification to provide a convenient and stable means to create a hydrophobic ceramic surface and tailor the effective pore size (Miller and Koros 1990; Caro et al. 1998; Castricum et al. 2005; Javaid et al. 2001; Abidi et al. 2006; Hyun et al. 1996; Leger et al. 1996; Randon and Paterson 1997). Alkyl, chloro-alkyl, or fluoro-alkyl silanes of varying carbon chain lengths can be used to provide chemical affinity, to improve the separation performance, and to provide a specific degree of pore size reduction (Javaid et al. 2001). The prepared membranes were grafted using two different organo-silane compounds, namely octyltrichlorosilane and γ-aminopropyl-trimethoxysilane, to select the appropriate one for the process. The membrane samples were immersed in the silane solution of different concentrations (2, 5, and 10 vol.% in ethanol) at room temperature (25°C) and then dried at 70°C for 24 h. The procedure was repeated twice for different time intervals: 24 and 72 h, giving a total of 96 h of immersion time. This procedure was used to characterize hydrophobicity and also grafting efficiency. After the immersion, the membranes were rinsed with ethanol two times to remove any unreacted chemicals from the membranes and dried at 70°C for 24 h. Finally, the membranes were stored at room temperature ready for characterization (Krajewski et al. 2006).

Methods for characterization

Thermal analysis, comprising both differential scanning calorimetry (DSC) and thermogravimetric analysis (TGA),

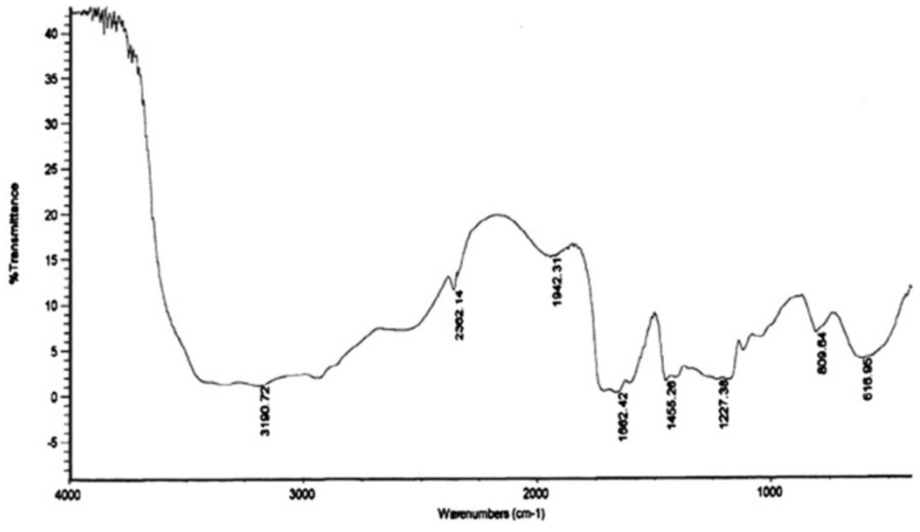

Figure 6 FTIR spectrum of the acrylic-acryl amide copolymer.

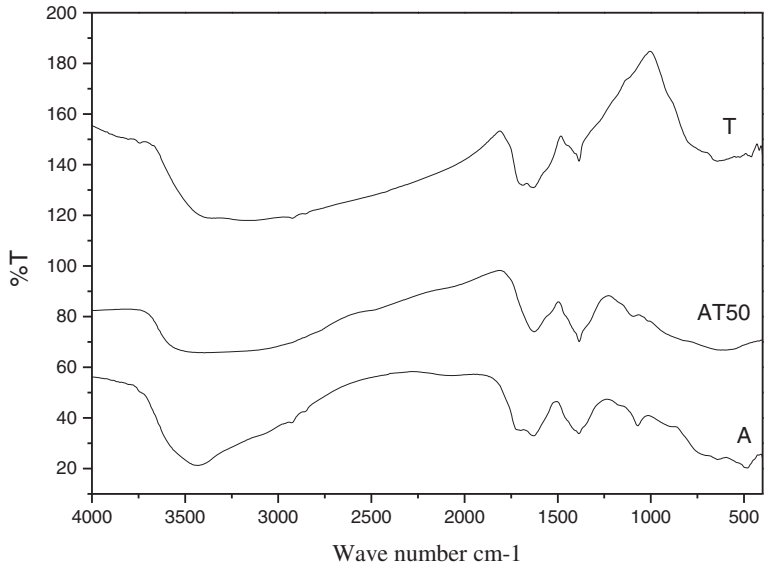

Figure 7 FTIR spectra of different gels of alumina (A), titania (T), and alumina-titania (AT50).

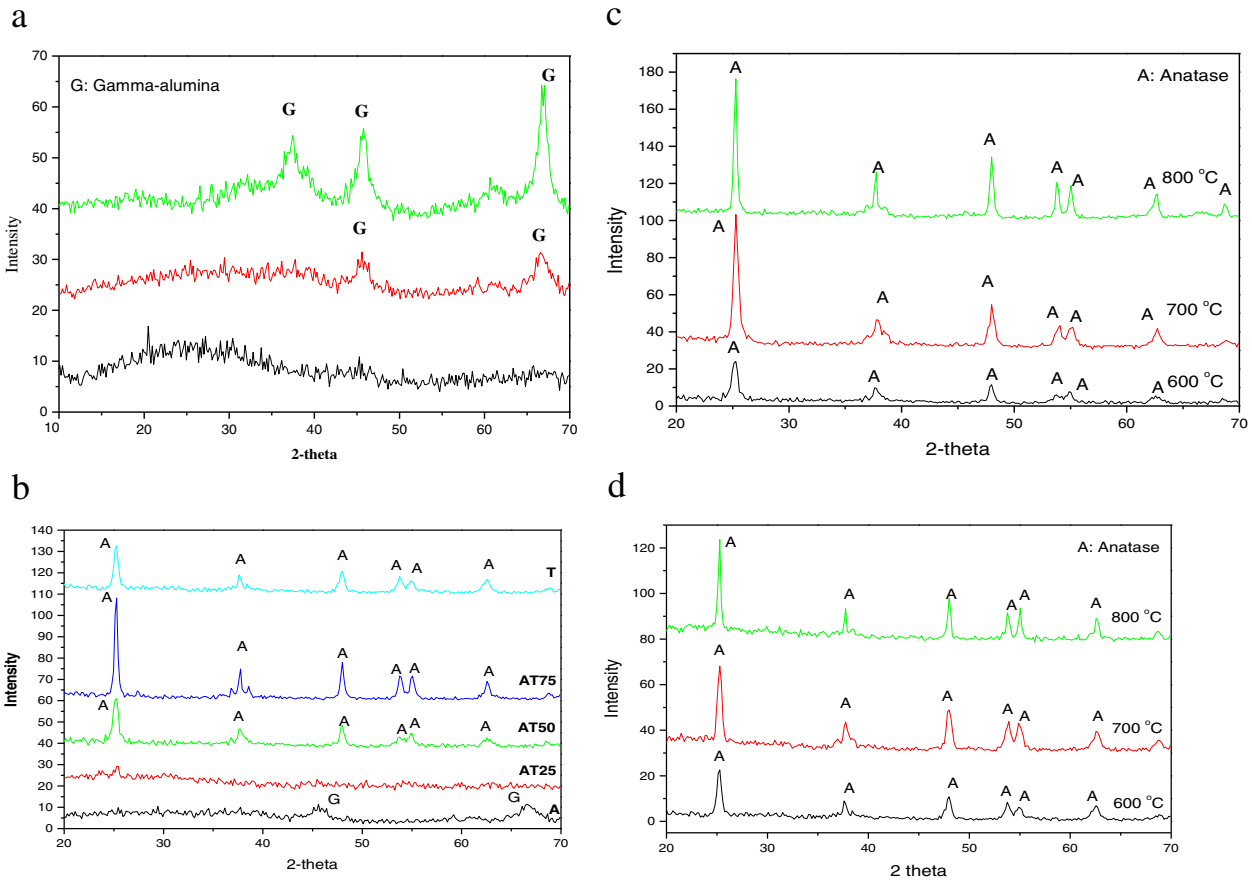

Figure 8 XRD patterns of the samples. (a) Alumina (A) powder calcined at 600°C, 700°C, and 800°C. **(b)** Alumina (A), alumina-titania (AT25, AT50, and AT75), and titania (T) membranes calcined at 700°C, where G is gamma-alumina and A is anatase. **(c)** Alumina-titania (AT50) membrane calcined at 600°C, 700°C, and 800°C. **(d)** Titania (T) membrane calcined at 600°C, 700°C, and 800°C.

was carried out on the acrylic-acrylamide copolymer and the dried membranes using a Setaram Labsys TM TG-DSC16 system (Newark, CA, USA).

Fourier transform infrared (FTIR) spectroscopy equipment (MB154S, Bomem, Quebec, Canada) was used to determine the main bonds in the copolymer and the effect of the introduced inorganic cations to the polymer structure on the spectra of the different groups.

X-ray diffraction analysis was carried out to characterize the respective alumina and titania phases developed in the membrane powder calcined at 600°C, 700°C, and 800°C utilizing Bruker D8 (Madison, WI, USA) and Cu Kα radiation. Scanning was carried out at a rate of 1° per minute in the 2θ range between 5° and 70°.

The surface area measurements were performed using Quantachrome Instruments NOVA Automated Gas Sorption version 1.12 (Boynton Beach, FL, USA). N_2 isotherms were performed at 77 K using a Coulter SA3 analyzer (Fullerton, CA, USA). The respective surface area values were calculated using the Brunauer-Emmett-Teller (BET) equation.

A transmission electron microscope (model JEOL JEM-1230, Akishima-shi, Japan) was used to examine the membrane powders with respect to their particle size and shape.

The distribution of pore size, pore area, and pore volume developed in the prepared membranes was determined using a Hg porosimeter (Type No. 9810). The chamber was first evacuated to a pressure less than 10 psia and then subjected to the introduction of a non-wetting liquid (mercury), under a hydraulic pressure of 14 to 415 Pa, corresponding to pore radii from approximately 2 nm to approximately 200 μm.

The morphological characteristics of the membrane surface and the thickness of the prepared layer after and before the grafting process were examined using scanning electron microscopy (SEM) equipment (Philips XL30, Amsterdam, The Netherlands). The method is based on directing a fine-focused electron beam accelerated under a maximum potential difference of 30 kV to scan the surface and microstructure of the specimen displayed on a cathode ray screen. The microstructure is then photographed at a magnification between × 200 and × 50,000.

The surface of the prepared membranes was treated to produce a kind of surface modification to maximize its degree of hydrophobicity by eliminating the existence of small, hydrophilic pores. This approach has been achieved through the treatment with chloro-alkyl silanes that enhanced surface flow and solution diffusion.

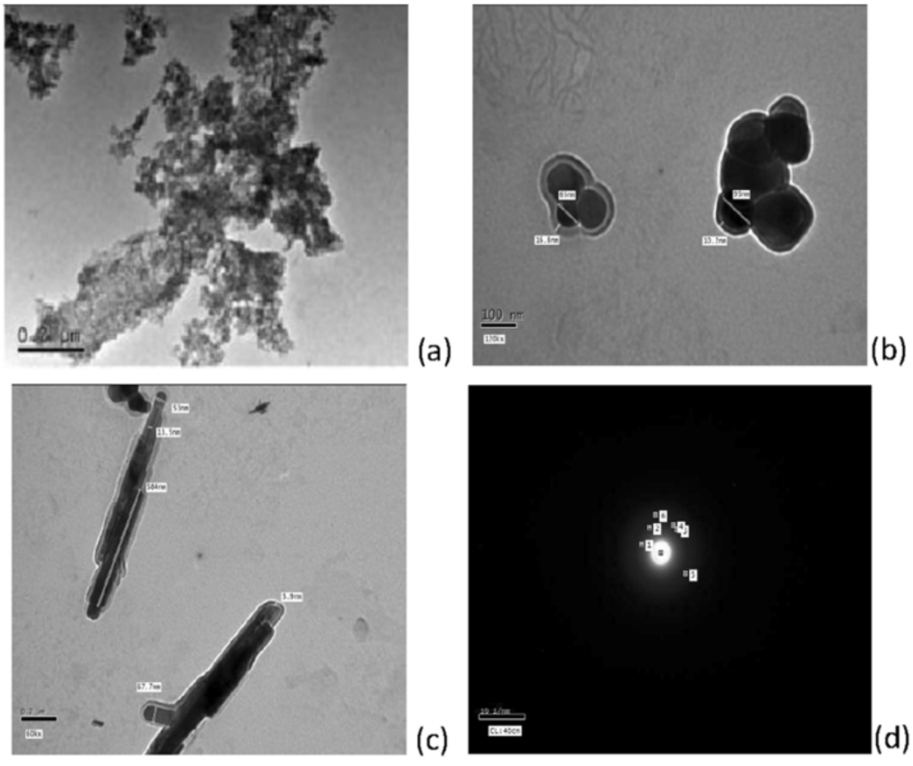

Figure 9 TEM images (a, b, c) and electron diffraction pattern (d) of the alumina (A) membrane powder fired at 700°C.

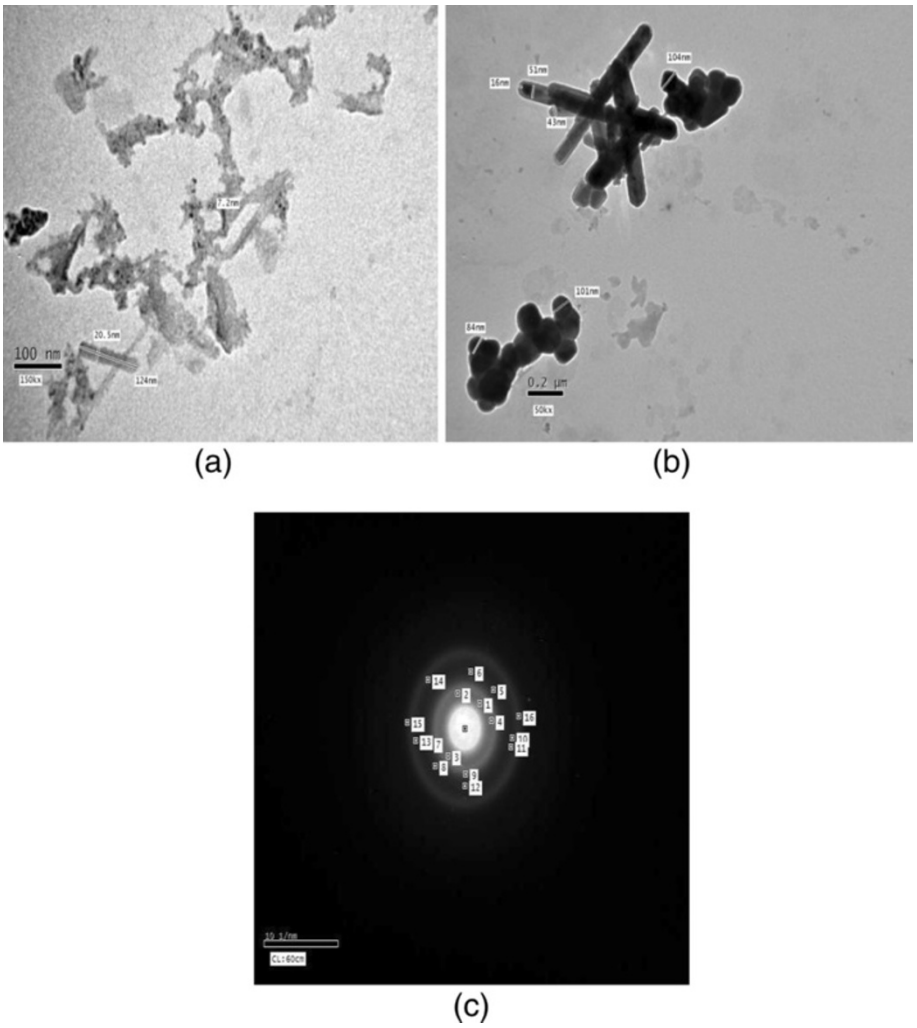

Figure 10 TEM images (a, b) and electron diffraction pattern (c) of the alumina-titania (AT50) membrane powder fired at 700°C.

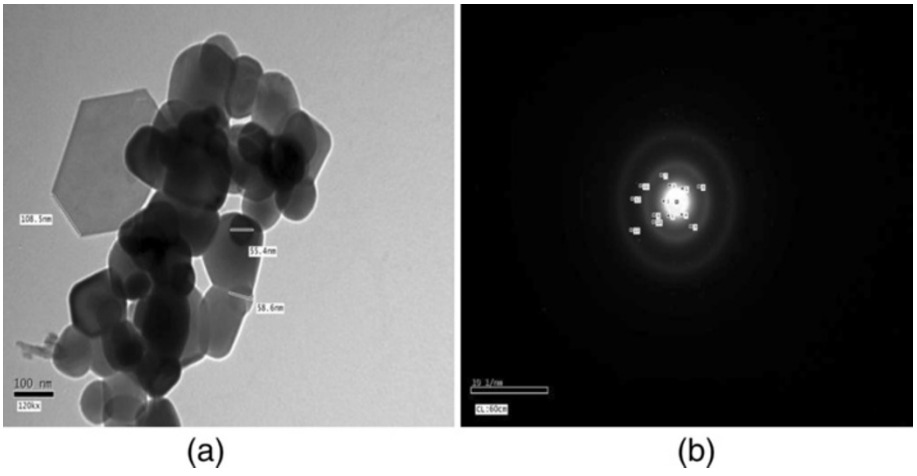

Figure 11 TEM image (a) and electron diffraction pattern (b) of the titania (T) membrane powder fired at 700°C.

The hydrophobic character of the prepared membranes was checked by measuring the contact angles of a sessile waterdrop on the membrane samples using a goniometer apparatus (Figure 2).

Water flux, permeability measurements, and salt rejection efficiency of the prepared membranes were performed using a homemade pilot plant, as shown in Figure 3.

The salt rejection efficiency of the prepared membranes was measured using a Hanna model conductivity electrode (model: HI99301). The retention coefficient (R_{NaCl}) was calculated according to the following equation:

$$R_{NaCl} = \{[CF_{NaCl} - CP_{NaCl}]/CF_{NaCl}\} \times 100\%,$$

where CF and CP denote the concentration of NaCl in both feed and permeate, respectively.

The desalination experiments were performed using the different prepared flat membranes, namely alumina (A), alumina-titania composite (AT25, AT50, AT75), and titania (T). A fixed flow rate (10 ml/s) and vacuum pressure (–0.8 bar) were used in the process. Three aqueous NaCl feed solutions were as follows: 2,000, 3,000, and 5,000 ppm.

The NaCl solutions were prepared and heated at different temperatures (45°C, 55°C, 65°C, and 75°C). The salt concentration of the permeate was measured in order to determine the respective retention coefficient. The temperature of the cooling condenser was maintained at 7°C.

Results and discussion

Thermal analysis

The TGA and DSC of the acrylic-acrylamide copolymer alone and those incorporated with Al^{3+} or Ti^{4+} cations are shown in Figures 4 and 5, respectively. Weight loss and destruction of the acrylic-acrylamide copolymer take place in three steps: loss of water (moisture) followed by a gradual dissociation of the copolymer that ends by the combustion of the copolymer at 450°C.

The DSC of the copolymer reveals four endothermic peaks. The glass transition temperature of the copolymer is at 85°C, followed by its melting point at 217°C. The third and fourth peaks at 334°C and 389°C, respectively, are due to dissociation of the copolymer according to the polymer molecular weight. Decomposition of the copolymer occurs as an exothermic peak at 420°C.

Figure 5a,b,c and Tables 2 and 3 show the TGA and DSC of the acrylic-acrylamide copolymer incorporated with alumina, titania, and alumina-titania composite, respectively. It was found that the thermogram of the acrylic-acrylamide copolymer incorporated with alumina, titania, and alumina-titania composite represents three stages of weight loss, as demonstrated before and illustrated in Table 3.

From Figure 5a, the glass transition temperature increased to 102°C and the softening point increased to 206.5°C. Also, the polymer was completely degraded at 508°C. Figure 5b shows that the glass transition temperature and the softening point of the acrylic-acrylamide copolymer coupled at 106.1°C, and the polymer was completely combusted at 570°C. Figure 5c shows that the glass transition temperature and the softening point of the acrylic-acrylamide copolymer were at 117.9°C and 232.2°C, respectively, while the polymer was combusted at 478.8°C.

It is clear that all reaction temperatures: glass transition, softening point, and combustion, of the copolymer are shifted to higher temperatures. These increases are due to the reaction that occurred between the metal oxide and copolymer.

Table 4 Surface area measurements for the different membrane powders calcined at 700°C

Sample ID	Type of membrane	Temperature (°C)	Surface area (m^2/g)	Particle size (nm)
A	Alumina (100 mol%)	700	481.2	3.28
AT25	Alumina (75 mol%)-titania (25 mol%)	700	333	4.63
AT50	Alumina (50 mol%)-titania (50 mol%)	700	201.9	7.69
AT75	Alumina (25 mol%)-titania (75 mol%)	700	175.1	8.81
T	Titania (100 mol%)	700	324.9	4.98

Fourier transform infrared spectroscopy

The IR spectrum of the acrylic-acrylamide copolymer is displayed in Figure 6. A broad band occurs at 2,500 to 3,500 cm^{-1} which is due to the combination of two broad bands corresponding to the stretching vibration of the amide group and the stretching vibration of the carboxylic group. The main bands corresponding to the presence of the C = O group occur at 2,362 and 1,662 cm^{-1}. The bending vibrations of O-H and N-H

Table 5 Results of the surface area of the alumina membrane powders calcined at 600°C, 700°C, and 800°C

Sample ID	Type of membrane	Temperature (°C)	Surface area (m^2/g)	Particle size (nm)
A	Alumina (100%)	600	812	1.89
A	Alumina (100%)	700	481.2	3.28
A	Alumina (100%)	800	282.7	5.99

Table 6 Pore size distribution of the different membranes

Sample symbol	Total intrusion volume (ml/g)	Total pore area (m^2/g)	Bulk density (g/ml)	Average pore diameter (μm)	Apparent density (g/ml)	Total porosity (%)
Support	0.2025	4.863	0.0914	2.2924	4.2786	46.42
Hydrophobic support	0.1756	4.087	0.1719	2.3728	4.0677	41.67
Intermediate layer	0.1547	3.116	0.2163	2.4669	3.9889	38.16
A	0.0951	9.080	2.9666	0.0419	4.1316	28.27
AT25	0.0785	24.258	2.7355	0.0129	3.4830	21.46
AT50	0.0971	8.273	2.9119	0.0248	4.0595	28.27
AT75	0.0344	5.546	2.9833	0.0469	3.3249	34.32
T	0.0998	35.464	2.5678	0.0113	3.3425	25.03

groups attached to the polymer are found at 1,027 and 810 cm^{-1}, respectively, while the main bands related to the rocking and bending vibrations of the C-H bond are detected at 617 and 1,455 cm^{-1}.

The IR spectra of the acrylic-acrylamide copolymer gels dried at 80°C, incorporated with one or two cations, e.g., Al^{3+}, Ti^{4+}, and Al^{3+}-Ti^{4+}, are shown in Figure 7.

The high-frequency part of the spectrum is dominated by a broad band occurring between 3,000 and 3,500 cm^{-1} which is a characteristic of the -OH stretching mode of -COOH groups in the 'acrylic-acrylamide copolymer' template polymer. The corresponding deformation modes appear in the range of 1,384 to 1,388 cm^{-1}.

The IR spectra of the substituted cations with the functional groups of the template polymer are more or less similar with only slight variation. This indicates that the same reactions between the metal oxide and copolymer are taking place.

The bands at the range 624 to 659 cm^{-1} in the substituted copolymer spectra are attributed to the different inorganic cations' R^+-(O-C)- stretching vibrations, where $R^+ = Al^{3+}$ and Ti^4.

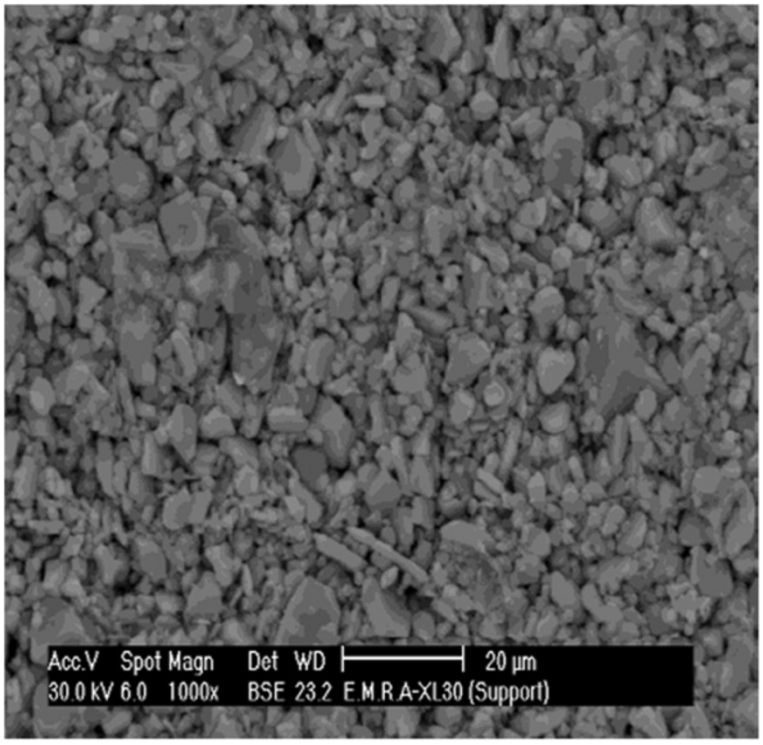

Figure 12 SEM image of the alumina support.

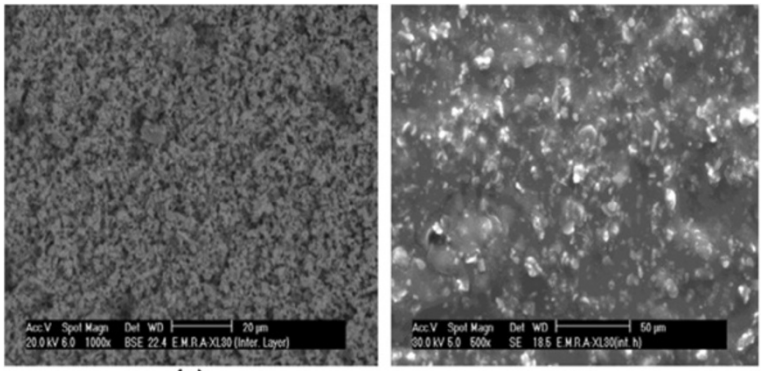

Figure 13 SEM images of both the (a) non-grafted and (b) grafted alumina intermediate layer.

The bands detected at 1,627 to 1,631 cm^{-1} correspond to the stretching mode of the C = O functional group, whereas the NH and OH stretching vibrations occur in the same range 3,300 cm^{-1}. Therefore, these bands failed to be distinguished from one another.

X-ray diffraction analysis

The X-ray diffraction (XRD) patterns of the different samples prepared using different molar ratios of the inorganic precursors ($AlCl_3$ and $TiCl_4$) added to the template polymer (acrylic-acrylamide copolymer) and subjected to a calcination reaction at temperatures between 600°C and 800°C for 3 h are displayed in Figure 8a,b,c,d.

The XRD patterns of the alumina (A) powders heat-treated at different temperatures: 600°C, 700°C, and 800°C, were ill crystalline at 600°C, whereas the γ-alumina phase started to appear at 700°C showing an increase in the peak intensity at 800°C, as shown in Figure 8a.

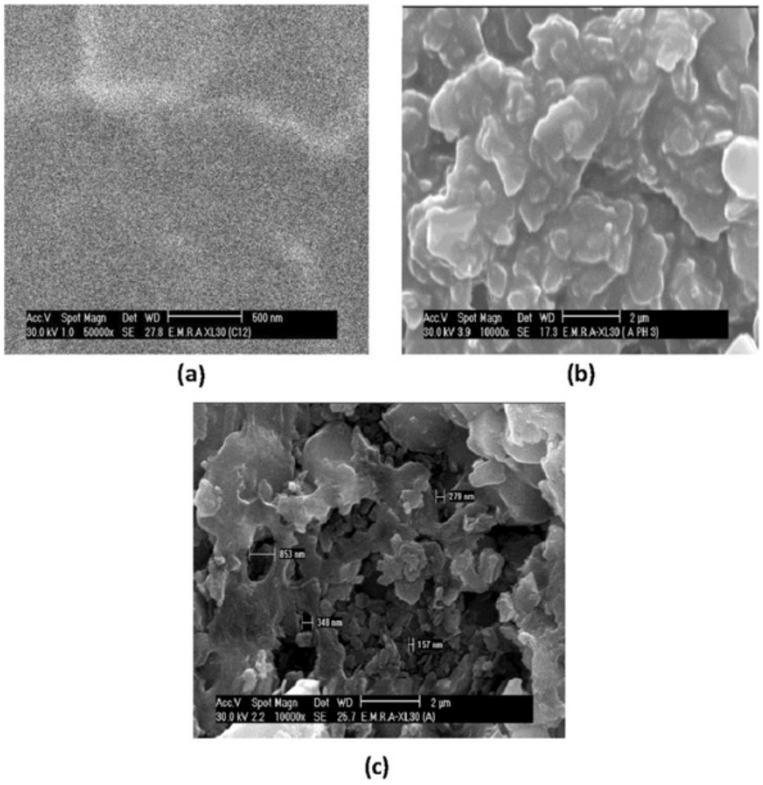

Figure 14 SEM images of the alumina membranes calcined at different temperatures: (a) 600°C, (b) 700°C, and (c) 800°C.

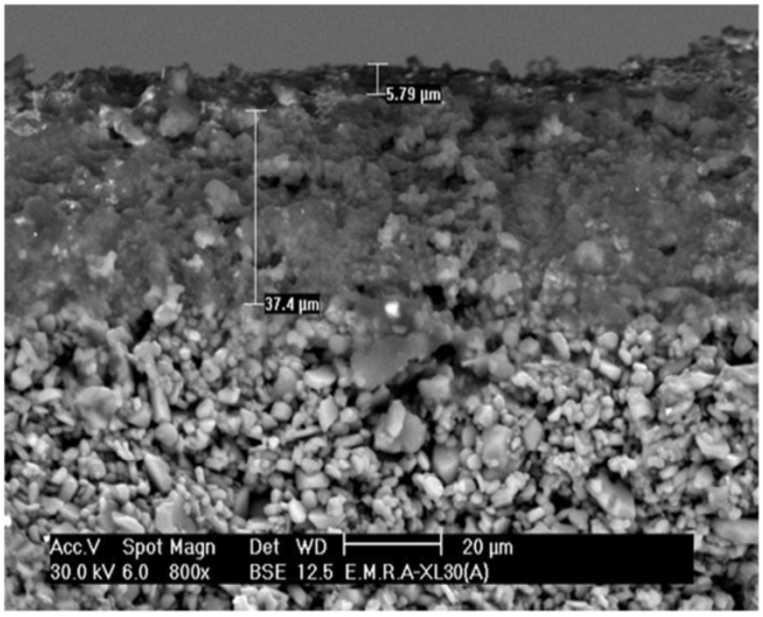

Figure 15 Cross section of the alumina membrane calcined at 700°C.

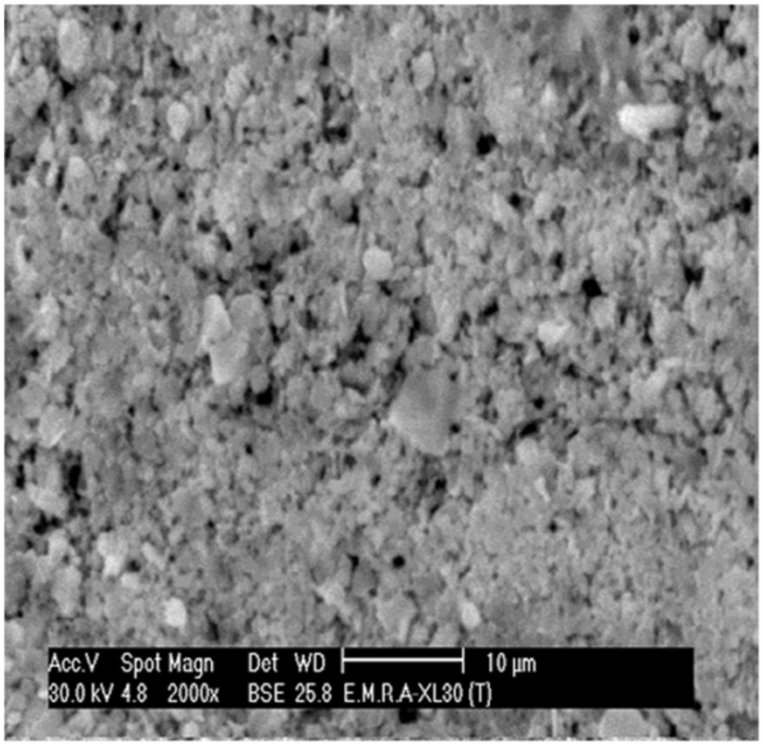

Figure 16 Titania membrane calcined at 700°C.

The XRD patterns of the membrane powders formed by alumina (A), alumina-titania (AT25, AT50, and AT75), and titania (T) were heat-treated at 700°C are shown in Figure 8b. The XRD pattern of alumina indicates a small peak depicted at $2\theta = 67°$ denoting the start of formation of the γ-alumina phase.

The XRD patterns of alumina-titania with different molar ratios of $AlCl_3/TiCl_4$: 75%:25%, 50%:50%, and 25%:75%, exhibit a characteristic peak at $2\theta = 25°$, attributed to the anatase phase beside that of γ-alumina. The intensity of the anatase peak increases with the increase of the proportion of titania concentration; as a result, the crystallization of the γ-alumina phase is retarded.

The XRD patterns of the alumina-titania (AT50) powders heat-treated at different temperatures are shown in Figure 8c. The alumina is ill crystalline at 600°C, with the start of formation of the γ-alumina phase at 700°C and 800°C. On the other hand, the titania crystallized as anatase in all powders heat-treated at 600°C up to 800°C. The peak intensity increases with the increase of the temperature of the treatment.

The XRD patterns of the titania (T) powders in Figure 8d show the anatase phase at 600°C up to 800°C. The intensity of the anatase peaks increases with the increase of the temperature of the treatment.

Transmission electron microscopy

Figures 9, 10, and 11 demonstrate the shapes of particles and overall appearance based on transmission electron microscopy of the prepared alumina, titania, and alumina-

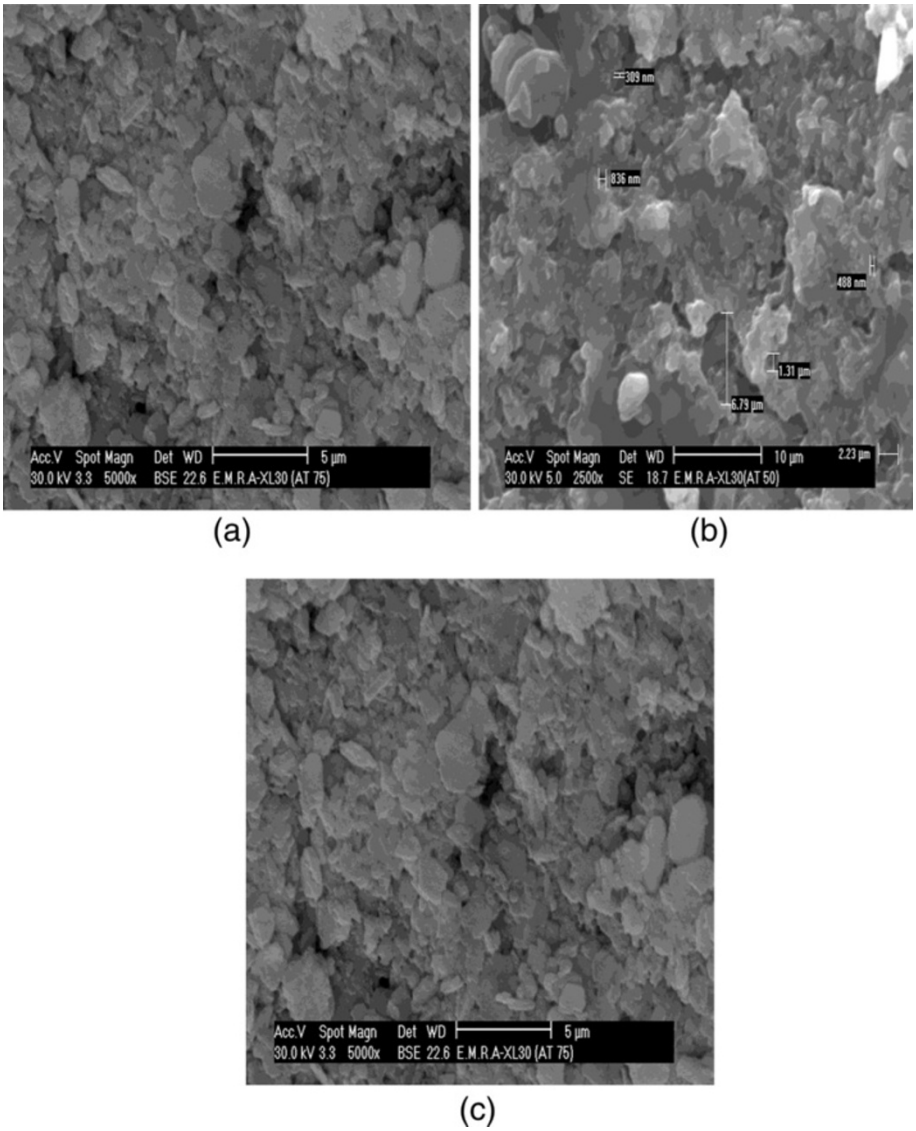

Figure 17 Alumina-titania composite membranes with different concentrations calcined at 700°C. (a) Alumina (75 mol%)-titania (25 mol%) (AT25) membrane. **(b)** Alumina (50 mol%)-titania (50 mol%) (AT50) membrane. **(c)** Alumina (25 mol%)-titania (75 mol%) (AT75) membrane.

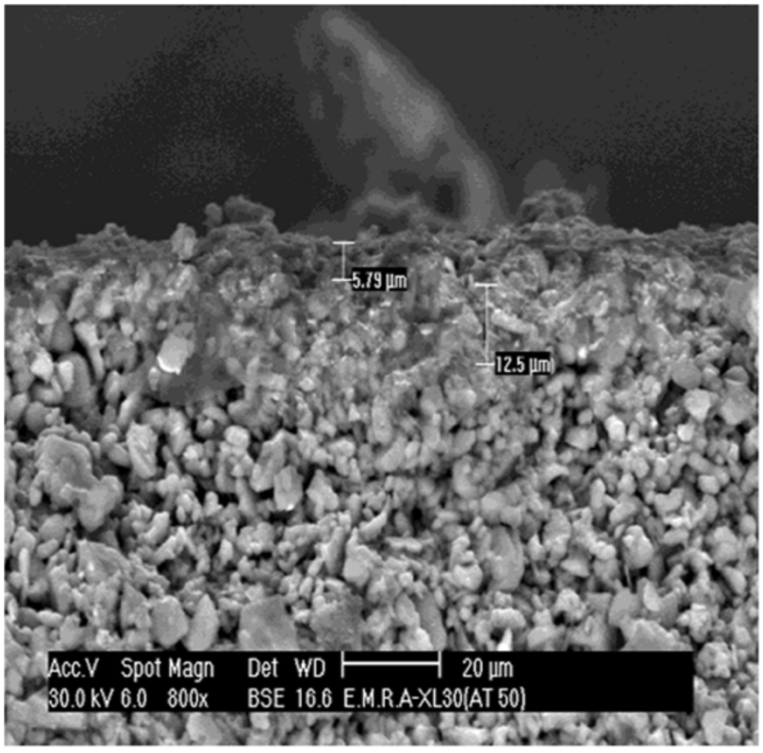

Figure 18 Cross section of the alumina-titania composite (AT50) membrane calcined at 700°C.

titania composite membrane powders heat-treated at 700°C for 3 h.

The TEM images of the alumina powder are shown in Figure 9a,b,c,d. Figure 9a shows a kind of agglomeration of the grains. The structure of the template polymer precursor was preserved by the substitution of the alumina cation as evident from the scattered dendrites. Figure 9b,c shows that the shape of the alumina grains ranged between spherical and rodlike with a size ranging from 65 to 95 nm. The electron diffraction pattern of the powder showed diffuse rings indicating the ill-crystalline nature of the grains with the presence of some spots presenting γ-alumina as demonstrated in Figure 9d.

The TEM images and electron diffraction pattern of the alumina-titania composite (AT) powder are shown in Figure 10a,b,c. The grains are agglomerated and arranged in a manner preserving the previous structure of the polymer, as demonstrated in Figure 10a, with a size ranging between 7 and 125 nm indicating the very fine nature of the powder. Figure 10b shows the shape of the particles that ranged between spherical and rodlike, with a size ranging between 16 and 104 nm. On the other hand, the electron diffraction pattern of the powder shows the presence of diffuse rings attributed to the amorphous nature of the alumina, besides the presence of spots indicating the anatase phase of titania, as shown in Figure 10c.

The TEM image and electron diffraction pattern of the titania (T) membrane powder in Figure 11a,b show agglomerates of the nano-grains with a size ranging

Table 7 Contact angle measurements of the alumina support modified with two different silane agents: C3 and C8

Number	Sample ID	Concentration of silane/ethanol solution (vol.%)	Side	CA (deg)	Average time (s)
1	C3 (2 vol.%)	2	Front	86.2	
			Back		8
2	C3 (5 vol.%)	5	Front		5
			Back		5
3	C3 (10 vol.%)	10	Front		6
			Back		11
4	C8 (2 vol.%)	2	Front	102.2	
			Back	115.7	
5	C8 (5 vol.%)	5	Front	116.3	
			Back	111.5	
6	C8 (10 vol.%)	10	Front	107.4	
			Back	106.1	

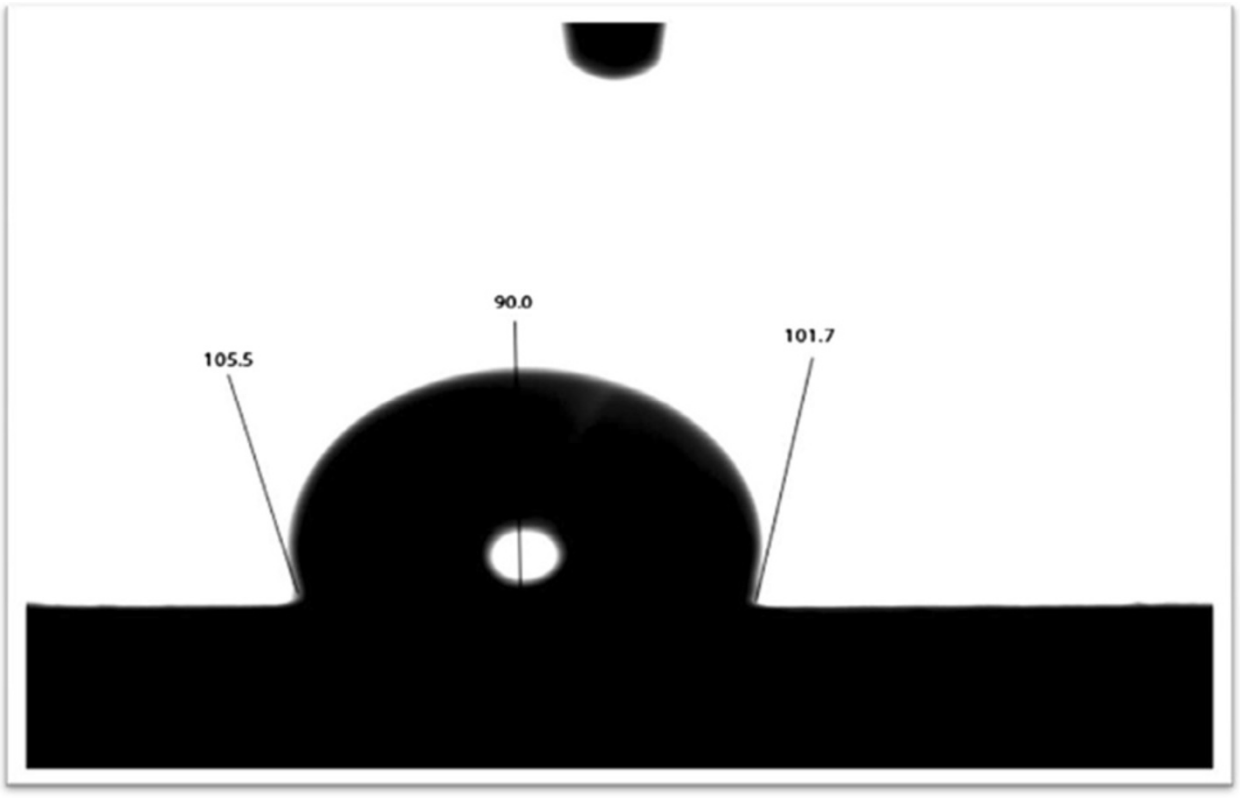

Figure 19 The waterdrop view on the hydrophobic surface of sample number 6 (one test).

between 55 and 108 nm indicating the fine nature of the powder. Particles are either spherical or hexagonal shaped. The electron diffraction pattern of the titania powder shows spots indicating the crystallization of the anatase phase.

Specific surface area

The results of the different membrane powders obtained after firing at 700°C in Table 4 indicate that the values of the specific surface area are affected by the type and molar ratio of the inorganic precursors reacted with the copolymer.

Powders of the alumina membranes heat-treated at 600°C, 700°C, and 800°C gave the following values for the specific surface area: 812, 481, and 282.7 m^2/g, respectively, whereas the calculated particle sizes were 1.89, 3.198, and 5.889 nm, as shown in Table 5.

Powders of the alumina-titania composite heat-treated at 700°C showed a decrease in the values of the specific surface area with the increase in the concentration of titania precursors. Coarsening of the grains took place as evident from the calculated values recorded which increased from 4.6318 to 8.813 nm, as shown in Table 4.

Pore size distribution

The porosity and pore size distribution measurements of the prepared membranes are greatly affected by the alumina-titania ratios while those modified by octyltrichlorosilane show a slight decrease in the respective porosities and pore size measurements, as demonstrated in Table 6. This indicates that the organo-silane agent does not affect the whole structure, but only affect the surface properties.

The change in the average pore diameter of the support on grafting recorded was between 2.29 and 2.37 μm and accompanied by a decrease in the total porosity from 46.42% to 41.67%.

The recorded pore diameters of the alumina (A), alumina-titania (AT25, AT50, and AT75), and titania (T)

Table 8 Wetting angle measurements for the different grafted membranes

Membrane ID	Contact angle (deg)
A	Approximately 119
AT50	Approximately 120
T	Approximately 123

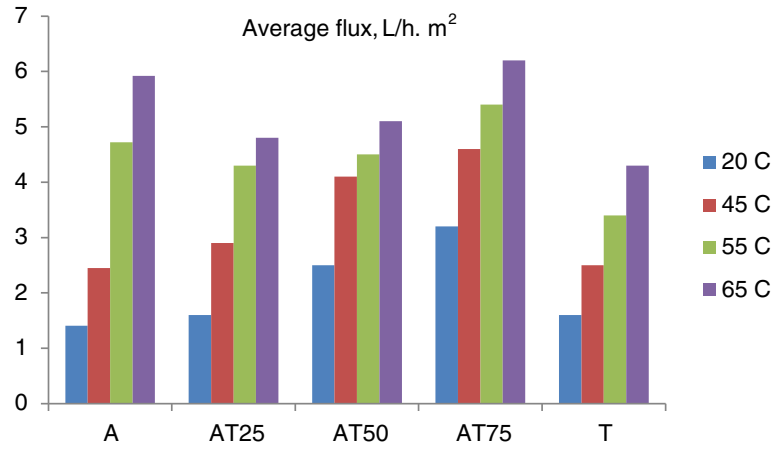

Figure 20 Permeate flux of water through the alumina, alumina-titania, and titania membranes at different temperatures.

membranes are in the following sequence: 41.9, 12.9, 46.9, 24.8, and 11.3 nm, with respective porosity of 21.46%, 28.27%, 34.32%, and 25.03%.

Scanning electron microscopy

Microstructures of the main layers as well as the cross sections of the prepared membranes are shown in Figures 12, 13, 14, 15, 16, 17, and 18.

The SEM image in Figure 12 shows the surface of the alumina support specimen fired at 1,400°C. The alumina grains with a size between 3 and 5 μm show a coarse columnar to platy shape that is randomly oriented giving a porous microstructure with a rough and pitted surface. The interstices between the grains are filled with smaller ones about 1 to 2 μm.

The SEM images in Figure 13 show the outer surface of the grafted and non-grafted intermediate layer. The SEM image in Figure 13a shows the alumina support specimen covered with an α-alumina intermediate layer (non-grafted sample) and fired at 1,000°C. The coarse alumina grains are totally covered by the intermediate layer with a grain size ranging between 0.2 and 0.5 μm with connected pores giving a smooth surface. The SEM image in Figure 13b shows the alumina support specimen covered with α-alumina intermediate layer, fired at 1,000°C, and grafted using octyltrichlorosilane. The covering layer displays the details of the underlying structure. No distinct behavior was spotted on the grafted surface.

The SEM images of the composite and monophase membranes in Figures 14, 15, 16, 17, and 18 show the effect of controlling the temperature profile of heat treatment and the concentration of the second phase on the elimination of microcracks and pinholes in the produced membranes to reduce the stresses originating from the removal of volatiles and the accompanying shrinkage.

The alumina membrane treated at 600°C in Figure 14a shows uniform and discrete layers. Increasing the temperature to 800°C, as shown in Figure 14c, leads to the formation of pinholes and cracks with coarsening of the grains through the agglomeration of the alumina particles to reach a size ranging between 348 and 853 nm. Figure 14b, on the other hand, shows the improvement of the surface of the membrane layer heated at 700°C, where these defects were diminished as possible with the presence of large alumina particles.

The SEM image of the cross section of the alumina (A) membrane in Figure 15 shows two different layers on top of the support: an intermediate layer with a thickness of 37.4 μm followed by the alumina membrane layer with a thickness of 5.7 μm.

The SEM image of the titania membrane heat-treated at 700°C in Figure 16 shows the uniformity of the surface that completely covers the alumina support.

The effect of the addition of titania as a second component to form the composite membrane is shown in Figures 17 and 18.

Table 9 Permeate flux of water through the alumina, alumina-titania, and titania membranes at different temperatures

Temperature (°C)	Average flux (l/h m^2)				
	A	AT25	AT50	AT75	T
20	1.4	1.6	2.5	3.2	1.51
45	2.5	2.9	4.1	4.6	2.5
55	4.7	4.3	4.5	5.4	3.4
65	5.9	4.8	5.1	6.2	4.3

The effect of the content of titania in the composite on the uniformity of the membrane layer is shown in Figure 17. A uniform surface of the alumina-titania composite (AT25) membrane heat-treated at 700°C is shown in Figure 17a. AT50 and AT75, on the other hand, show a kind of non-uniformity that might be generated by the stresses arising from the start of conversion of anatase to rutile phase, and this conversion is usually accompanied by grain growth of the latter phase, as shown in Figure 17b,c.

The SEM cross-sectional image of the alumina-titania composite (AT50) membrane as an example of the alumina-titania composite samples is shown in Figure 18. Two different layers appear on top of the support. The support is covered by an intermediate layer with a thickness of 12.5 μm followed by the alumina-titania composite membrane layer with a thickness of 5.7 μm.

The SEM image of the surface of the alumina-titania (AT25) membrane showed a uniform crack-free top layer with the least pore diameter of 0.0129 μm as demonstrated from the pore size distribution results.

Contact angle measurements

In the present work, two different organo-silane compounds, namely γ-aminopropyl-trimethoxysilane (C3) and octyltrichlorosilane (C8), were selected to carry out the surface modification.

The grafted membranes (alumina (A), alumina-titania composite (AT), titania (T)) obtained by immersion in a silane solution of different concentrations (2, 5, and 10 vol.%) in an ethanol solution at room temperature 25°C were tested by measuring the contact angle developed on the surface. Also, these membranes were subjected for water permeation and water desalination. Therefore, the degree of water permeability and the rejection coefficient (*R*%) of the modified membranes were measured.

The results obtained shown in Table 7 represent an average of three readings for the tested membranes. An example of the drop formation and testing measurements is demonstrated in Figure 19.

The measured contact angles of the non-grafted supports are lower than 90°. Accordingly, they are considered hydrophilic and likely to absorb water. On the other hand, the measured contact angles of three alumina support samples grafted using γ-aminopropyl-trimethoxysilane denoted by C3 (2, 5, and 10 vol.%) are demonstrated in Table 7.

Accordingly, octyltrichlorosilane (C8, 5 vol.%) was selected to graft the prepared ceramic membranes for the desalination measurements including water flux and rejection coefficient (*R*%) measurements for each membrane.

Table 10 The retention coefficient values of NaCl solutions through alumina, alumina-titania, and titania membranes

NaCl concentration (ppm)	Feed/permeate temperature (°C)	Retention coefficient (%)				
		A	AT25	AT50	AT75	T
2,000	45:7	19.58	26.30	28.51	11.5	10.67
	55:7	21.57	29.56	31.77	17.11	27.54
	65:7	32.52	41.55	38.69	19.17	38.96
	75:7	35.24	46.55	42.77	30.52	42.93
3,000	45:7	26.2	28	30.79	15.31	24.27
	55:7	45.24	36.22	39.10	28.11	43.69
	65:7	47.62	44	46.43	29.32	53.79
	75:7	50.82	47.25	48.88	30.67	58.09
5,000	45:7	34.44	53.02	32.99	16.87	53.58
	55:7	49.77	56.11	46.43	37.65	54.91
	65:7	51.39	63.58	60.49	40.09	56.23
	75:7	54.26	72.59	70.26	47.43	61.57

The wetting angles of the different grafted membranes using 5 vol.% octyltrichlorosilane (C8) indicated that the contact angle values recorded are independent of the membrane type as they show more or less the same contact angle, as shown in Table 8.

Vacuum membrane distillation experiments

Water permeation process

The measured values of water flux through the prepared membranes depend on the temperature difference between the feed and permeate sides, as shown in Figure 20. Thus, the alumina membrane showed a gradual increase in water flux from 1.4 to 3.9 l/h m^2 when the temperature was raised gradually from 20°C to 65°C.

The results in Table 9 compare water fluxes through the different grafted membranes (alumina (A), alumina-titania (AT25, AT50, AT75), titania (T)). It is evident from these results that water flux slightly depends on the pore diameter of the used membrane. The water fluxes of 1.58 and 1.5 l/h m^2 measured at 20°C were recorded through the AT25 and T membranes with an average pore diameter of 12.9 and 11.3 nm, respectively.

These values were smaller than those reported for other alumina (A) and alumina-titania composite types

Table 11 Comparison between values of retention coefficient of NaCl solution (5,000 ppm at 75°C) using the different membranes

	Membrane type				
	A	AT25	AT50	AT75	T
Retention coefficient (%)	54.26	72.59	70.26	47.43	61.57

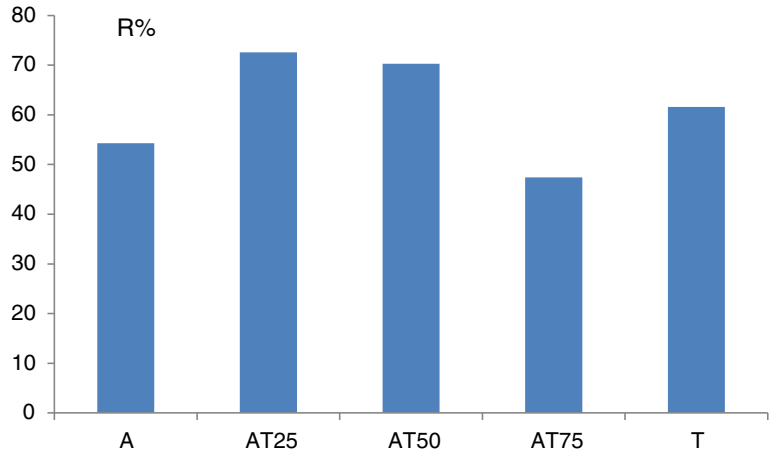

Figure 21 Comparison between retention coefficient values of NaCl solution (5,000 ppm at 75°C) using the different membranes.

(AT50 and AT75) of 4, 2.5, and 4.2 l/h m^2 measured at 20°C with an average pore diameter of 41.9, 24.8, and 46.9 nm, respectively.

Desalination process

The retention coefficient values (*R*%) of the different grafted membranes are presented in Table 10 which depended strongly on the temperature difference between the feed and the permeate side and on the concentration of the NaCl solution. The alumina membrane shows a retention coefficient of 34, 49.7, 51.39, and 54.26 at a temperature difference of 45:7, 55:7, 65:7, and 75:7, respectively.

The retention coefficient values (*R*%) showed an increase by increasing the concentration of the NaCl solution. The retention coefficient (*R*%) of the alumina membrane increased from 35.24% to 54.2% by increasing the NaCl solution concentration from 2,000 to 5,000 ppm.

The alumina-titania composite (AT25 and AT50) and titania (T) membranes showed a higher ability to reject the NaCl salt from water showing a retention coefficient of 72.59%, 70.26%, and 61.57%, respectively, while the alumina-titania composite AT75 showed a lower retention coefficient of 47.43%.

Figure 21 and Table 11 show the salt retention (R_{NaCl}) during the membrane distillation process using the different grafted membranes (A, AT25, AT50, and T) at the temperature difference of 75:7 using NaCl solution of 5,000 ppm as a feed solution. It can be seen that the salt retention coefficient in the MD process with the different prepared grafted membranes is close to 75%. This can be explained by the fact that some of the biggest pores were wetted and limited transport of NaCl solution could occur.

Conclusions

The study of the preparation of membranes via the application of the acrylic-acrylamide copolymer as template was successful in overcoming the presence of cracks through the different additions. It was possible to obtain membrane layers of uniform nano-pore size and porosities between 25% and 37% fired at 700°C. The crystal and morphological structures of the alumina-titania membranes were affected by the $AlCl_3$ and $TiCl_4$ feed ratio. The addition of titania succeeded in hindering the crystallization of the alumina phases and eliminating the possibility of the accompanying cracking. The polymeric route using acrylic-acrylamide copolymer as a template polymer led to preparation of membranes with ill-crystalline nature at 600°C that started to crystallize at 700°C which showed high surface area values as well as nano-pore size and meso-porosities. The results of water permeation showed that there is an upper limit for the addition of titania. The final supported membranes prepared using alumina-titania (AT25 and AT50) precursors showed uniform layers without cracks. The alumina-titania composite (AT) membranes showed a pore size of 13 to 46 nm, porosity of 21% to 34%, and water permeability of 2 to 8 l/h m^2/bar. These membranes can be used for ultrafiltration purposes, such as pretreatment of water desalination and concentration of aqueous solutions (fruit juice, sugar solution). The polymeric sol–gel method used in this study to produce different hydrophobic alumina-titania membranes which utilized chloride salts of aluminum and titanium using acrylic-acrylamide as a template polymer and octyltrichlorosilane as a grafting agent is promising and can be used for different membranes.

Competing interests
The authors declare that they have no competing interests.

Authors' contributions
AMANY Gaber carried out the membrane prepration studies and drafted the manuscript. Doreya Ibrahim: participated in the design of the study and revese the manuscrpt. Fawzia Fahim: prepared the template polymer used in the study. Elham ELZANZTI: measure the permeability performance of the different prepared membranes. All authors read and approved the final manuscript

Author details
[1]Ceramic Department, National Research Centre, Cairo, Egypt. [2]Polymers Department, National Research Centre, Cairo, Egypt. [3]Chemical Engineering Department, National Research Centre, Cairo, Egypt.

Received: 7 May 2013 Accepted: 16 October 2013
Published: 01 Nov 2013

References

Abidi N, Sivade A, Bourret D, Larbot A, Boutevin B, Guida-Pietrasanta F, Ratsimihety A (2006) Surface modification of mesoporous membranes by fluoro-silane coupling reagent for CO_2 separation. J Membr Sci 270:101

Benfer S, Popp U, Richter H, Siewert C, Tomandl G (2001) Development and characterization of ceramic nanofiltration membranes. Sep Purif Tech 22 (23):231–237

Benfer S, Árki P, Tomandl G (2004) Ceramic membranes for filtration applications —preparation and characterization. Adv Eng Mater 6(7):495–500

Caro J, Noack M, Kolsch P (1998) Chemically modified ceramic membranes. Micropor Mesopor Mat 22:321

Castricum HL, Sah A, Mittelmeijer-Hazeleger MC, ten Elshof JE (2005) Hydrophobisation of mesoporous γ-Al_2O_3 with organochlorosilanes—efficiency and structure. Microspor Mesopor Mat 83:1

Gaber AA (2007) Preparation of alumina membranes by sol–gel polymeric route. M.Sc Thesis, Cairo University

Hyun SH, Jo SY, Kang BS (1996) Surface modification of γ-alumina membranes by silane coupling for CO_2 separation. J Membr Sci 120:197–206

Javaid A, Hughey MP, Varutbangkul V, Ford DM (2001) Solubility-based gas separation with oligomer-modified inorganic membranes. J Membr Sci 187:141

Krajewski SR, Kujawski W, Bukowska M, Picard C, Larbot A (2006) Application of fluoroalkylsilanes (FAS) grafted ceramic membranes in membrane distillation process of NaCl solutions. J Membr Sci 281:253–259

Kumar K-NP (1993) Nanostructured ceramic membranes; layer and texture formation. Ph.D. Thesis, University of Twente, Enschede, The Netherlands, p 113

Larbot A, Alami-Younssi S, Persin M (1994) Preparation of γ-alumina nanofiltration membrane. J Membr Sci 97:167

Leger C, Lira HDL, Paterson R (1996) Preparation and properties of surface modified ceramic membranes. Part III. Gas permeation of 5 nm alumina membranes modified by trichloro-octadecylsilane. J Membr Sci 120:187

Miller JR, Koros WJ (1990) The formation of chemically modified g-alumina microporous membranes. Sep Sci Technol 25:1257

Puhlfürß P, Voigt A, Weber R, Morbe M (2000) Microporous TiO_2 membranes with a cut off <500 Da. J Membr Sci 174:123

Randon J, Paterson R (1997) Preliminary studies on the potential for gas separation by mesoporous ceramic membranes modified by tri-chlorooctadecylsilane. J Membr Sci 120:187

Richter H, Piorra A, Tomandl G (1997) Developing of ceramic membranes for nanofiltration. Key Eng Mater 132–136:1715–1718

Schaep J, Vandecasteele C, Peeters B, Luyten J, Dotremont C, Roels D (1999) Characteristics and retention properties of a mesoporous γ-Al_2O_3 membrane for nanofiltration. J Membr Sci 163:229

Sekulic J, Magraso A, ten Elshof JE, Blank DHA (2004) Influence of ZrO_2 addition on microstructure and liquid permeability of mesoporous TiO_2 membranes. Micropor Mesopor Mat 72:49–57

Shojai F, Mantyla TA (2001) Chemical stability of yttria doped zirconia membranes in acid and basic aqueous solutions: chemical properties, effect of annealing and ageing time. Ceram Int 27:299–307

van Gestel T, Vandecasteele C, Buekenhoudt A, Dotremont C, Luyten J, Leysen R, van der Bruggen B, Maes G (2002) Alumina and titania multilayer membranes for nanofiltration: preparation, characterization and chemical stability. J Membr Sci 207:73

van Gestel T, Vandecasteele C, Buekenhoudt A, Dotremont C, Luyten J, van der Bruggen B, Maes G (2003) Corrosion properties of alumina and titania NF membranes. J Membr Sci 214:21

Wildman DL, Peterson RA, Anderson MA, Hill CG (1994) Investigation of titania membranes for nanofiltration. In: Proceedings of the ICIM94. Worcester Polytechnic Institute, Worcester, p 111

Xu Q, Anderson MA (1993) Sol–gel route to synthesis of microporous ceramic membranes: thermal stability of TiO_2–ZrO_2 mixed oxides. J Am Ceram Soc 76:2093–2097

Zhang H, Banfield JF (1999) Synthesis and applications of TiO_2 nanoparticles. Am Mineral 84:528.7.A

10.1186/2093-3371-4-18
Cite this article as: Gaber *et al.*: Synthesis of alumina, titania, and alumina-titania hydrophobic membranes via sol–gel polymeric route. *Journal of Analytical Science and Technology* 2013, 4:18